Single Molecule Spectroscopy of Conjugated Polymer Chains in an Electric Field-Aligned Liquid Crystal

Wei-Shun Chang,[†] Stephan Link,[†,§] Arun Yethiraj,*[,‡] and Paul F. Barbara*[,†]

Center for Nano- and Molecular Science and Technology and Department of Chemistry and Biochemistry, University of Texas at Austin, Austin, Texas 78712, and Department of Chemistry, University of Wisconsin, Madison, Wisconsin 53706

Received: August 7, 2007; In Final Form: September 6, 2007

Using single molecule polarization spectroscopy, we investigated the alignment of a polymer solute with respect to the liquid crystal (LC) director in an LC device while applying an external electric field. The polymer solute is poly[2-methoxy-5-(2′-ethyl-hexyloxy)-1,4-phenylene vinylene] (or MEH-PPV), and the LC solvent is 5CB. The electric field induces a change in the LC director orientation from a planar alignment (no electric field) to a perpendicular (homeotropic) alignment with an applied field of 5.5×10^3 V/cm. We find that the polymer chains align with the LC director in both planar and homeotropic alignment when measured in the bulk of the LC solution away from the device interface. Single molecule polarization distributions measured as a function of distance from the LC device interface reveal a continuous change of the MEH-PPV alignment from planar to homeotropic. The observed polarization distributions are modeled using a conventional elastic model that predicts the depth profile of the LC director orientation for the applied electric field. The excellent agreement between experiment and simulations shows that the alignment of MEH-PPV follows the LC director throughout the LC sample. Furthermore, our results suggest that conjugated polymers such as MEH-PPV can be used as sensitive *local* probes to explore complex (and unknown) structures in anisotropic media.

Introduction

Composite materials composed of mixtures of polymeric solutes and liquid crystalline solvents are of interest for a variety of reasons. The anisotropic solvent provides a means of controlling the conformation and orientation of polymer solutes, through solvent−solute interactions. It might therefore be possible to fabricate well organized nano and meso scale polymer structures with important optoelectronics applications.[1−4] For example, conjugated polymers have been synthesized using a liquid crystal (LC) template in order to enhance the electric properties of the polymer.[2,3] Recent studies have investigated the enhanced alignment of conjugated polymers in a nematic and smectic single LC. In this work we investigate the effect of an external electric field on the polymer alignment in a LC device.

A polymeric solute tends to align with the nematic director of the solvent. Single molecule spectroscopic studies have been used to measure the molecular details of the alignment of polymers dissolved in a LC matrix[5−8] and to show that the stiff conjugated polymer MEH-PPV dissolved in the nematic solvent 5CB is elongated and almost perfectly aligned with the nematic director.[6−9] This solvent-directed alignment of the polymer chains has been explained by a "cooperative solvation" model.[6−8] The MEH-PPV molecules, which are about 100 times larger than the 5CB solvent molecules, experience an effective mean solvation potential from a large number of solvent LC molecules, which "cooperatively" force the MEH-PPV to align parallel to the director. Onsager first predicted this phenomenon for a binary solution of long and short rods and found theoretically that in a nematic environment the long rods are highly aligned with the average alignment direction of the short rods (i.e., nematic director).[10] In this paper, we further explore the alignment of MEH-PPV in an LC solvent with different director orientations, which is achieved through electric field (E-field) induced switching of the orientation of the LC molecules.

The molecules in a nematic phase align in an externally applied E-field above a certain critical threshold voltage V_c.[11] Above V_c, LC molecules that have a dipole moment parallel to the long molecular axis and hence a positive dielectric anisotropy are attracted by the E-field. The opposite case holds for LC molecules with negative dielectric anisotropy. The transition to this E-field induced alignment of the LC molecules is known as the Frederick's transition,[11] and is often studied by electro-optical experiments.[12−15] Consider a device consisting of an LC solution sandwiched between two transparent electrodes. In the absence of an E-field the molecules align parallel to the surfaces in a planar alignment. When an E-field above V_c is applied in a direction perpendicular to the surfaces, the molecules are aligned parallel to the E-field, i.e., perpendicular to the LC device. This E-field-induced director alignment is referred to as homeotropic alignment. However, the molecules near the device interface remain aligned parallel to the substrate due to strong interactions (i.e., surface anchoring) with a surface alignment layer consisting typically of a polymer coating. The effect of an applied E-field on the local order of LC solvents is of interest in fundamental science and flat-panel display applications. The director orientation at the device interface has been measured by many techniques including optical[15−32] and

* Corresponding authors: E-mail: P.F.B., p.barbara@mail.utexas.edu; A.Y., yethiraj@chem.wisc.edu.
† University of Texas at Austin.
‡ University of Wisconsin, Madison.
§ Current address: Department of Chemistry, Rice University, Houston, TX 77005.

10.1021/jp076345m CCC: $40.75
Published on Web 11/02/2007

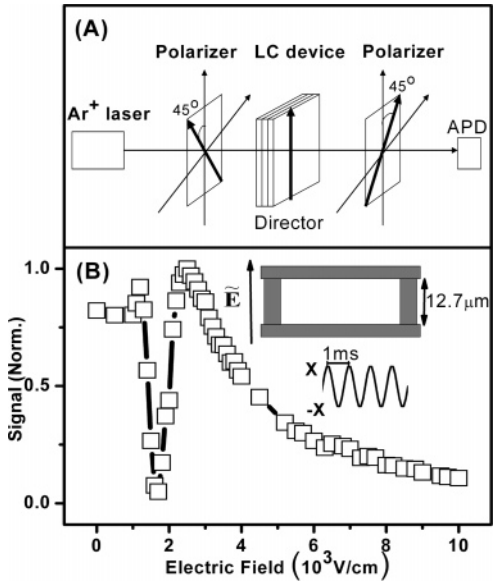

Figure 1. (A) Experimental setup for the electro-optical measurements. (B) Electro-optical response of 5CB in a nematic cell at room temperature. Inset: Schematic of the nematic cell and the function of the applied E-field.

acoustic[33−36] methods and has been explained by a elastic continuum theory.[11,37]

In this work, we use single molecule spectroscopy to investigate the orientation of MEH-PPV molecules in a nematic LC solvent with and without an applied E-field as a function of distance from the LC substrate interface. We find that the polymer molecules align with the director orientation in the planar and homeotropic case. In addition, for the homeotropic alignment, the experiments show a parallel alignment of polymers near the interface and a perpendicular alignment in the "bulk" region with a continuous change of polymer orientations between the two regions. This suggests that MEH-PPV can be used as a sensitive probe of the local order and dynamics in complex anisotropic media.

Experimental Section

Single nematic LCs of MEH-PPV (M_n = 110 000, Dr. Paul Burn from the University of Oxford, UK) in 5CB (Aldrich) with a concentration of $10^{-5}-10^{-8}$ % by weight are prepared starting from a polymer−5CB−chlorobenzene triphase system, as described previously.[8,9] After evaporation of the chlorobenzene, the MEH−PPV−5CB mixture is sandwiched between unidirectionally rubbed PVA alignment layers coated onto ITO coverslips separated by a 12.7 μm Mylar spacer. The director of the LC is determined by the rubbing direction. The formation of the nematic liquid crystalline phase is checked by the observation of birefringence under an optical microscope equipped with crossed polarizers (Zeiss Axioskop 2 Mat).

Electro-optical measurements are performed by using an incident laser beam of 488 nm passing through a front polarizer and then a nematic cell, followed by a rear polarizer (i.e., analyzer). The signal $I(V)$ is detected by an avalanche photodiode (APD, Perkin-Elmer SPCM), as shown in Figure 1(A). The analyzer and the nematic director of the LC are oriented 90° and 45° with respect to the front polarizer, respectively. The transmittance is measured as a function of applied electric field (AC, sinusoidal wave with frequency of 1 kHz).

Single molecule polarization experiments are performed on a home-built confocal microscope consisting of an inverted microscope (Zeiss Axiovert 200), a cw Ar ion laser (Melles Griot), and two APDs. Dual channel data acquisition of the fluorescence bursts is accomplished with a photon counter/multiscaler (Becker & Hickl PMS-400). The LC samples are mounted on a manual rotation and x-y translation stage. The rotation stage allows for convenient 360° sample rotation while the translation stage enabled probing different regions of the LC. The samples are excited with circularly polarized light at 488 nm, and the average power is about 100−200 nW which corresponds to 200−400 W cm^{-2} with a diffraction-limited spot size of 250 nm. The emission bursts are collected by the objective (Zeiss Fluar 100× oil immersion objective with a numerical aperture (NA) = 1.3) and are filtered by notch and long-pass filters in order to remove scattered laser light. Using a polarizing cube beamsplitter, the x- and y-components of the polarized emission (I_x and I_y) are detected by the two APDs. The detection scheme is set up in such a way that the x- and y-components are in the plane of the LC sample with the exciting laser light propagating in the z-direction. Polarization histograms are measured with or without an applied E-field of 5.5×10^3 V/cm (rms voltage) at various depths ranging between 0 and 3 μm away from the LC-PVA interface. All measurements are performed with the sample positioned so that the rubbing direction is parallel to the laboratory y-axis.

Histograms of single-molecule polarizations are generated using an automated routine. Dual channel fluorescence trajectories are acquired for 30−60 min for each sample orientation using a 10 ms bin time. The data is binned into 50 ms time intervals to create single bin bursts. After a background correction, all points below a threshold value are deleted. The threshold intensity to identify a fluorescence burst is set to three times the mean background. The polarization ratio, P, was calculated for each fluorescence burst and therefore one molecule at a time according to:

$$P = \frac{I_y - I_x}{I_y + I_x} \tag{1}$$

Polarization histograms are then generated consisting of several hundred fluorescence bursts for each measurement depending on the concentration of the sample and total acquisition time.

Results and Discussion

Electro-optical measurements are routinely employed to determine the orientation of LC molecules in a LC device with an applied E-field.[12−15,38] Figure 1(A) is a schematic drawing of the setup used for measuring the transmittance through a LC device positioned between two crossed polarizers. The LC director is oriented 45° with respect to both polarizers. Because of the birefringence of the LC molecules, transmittance is observed when LC molecules are aligned parallel to the substrate. In contrast, for LC molecules oriented perpendicular to the substrate, the transmittance decreases to zero because the absence of sample birefringence leaves the polarization of the incident light unchanged. Figure 1(B) shows the room-temperature electro-optical response of 5CB. In the absence of an E-field, the long axes of the LC molecules are aligned parallel to the surface due to the sample preparation method described in the Experimental Section. Above V_c = 1 V, the LC molecules start to align with the E-field because of the positive dielectric anisotropy of 5CB. The change of the LC director orientation in response to an increasing E-field alters the birefringence of the nematic cell and hence the observed transmittance. The transmittance vs applied field for 5CB, as shown in Figure 1(B), is consistent with previously published results.[38] At a voltage

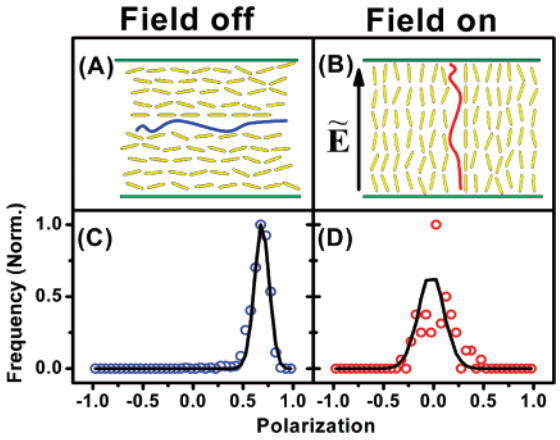

Figure 2. Top: Schematic picture showing the orientation of a nematic LC without (A) and with (B) an applied E-field. Solvation of large polymers (not scaled) is indicated by the blue (A) and red (B) chains. Bottom: Experimental polarization histograms (scatter) and corresponding fit (line) obtained without (C) and with (D) applied E-field at 3 μm from the LC−PVA interface.

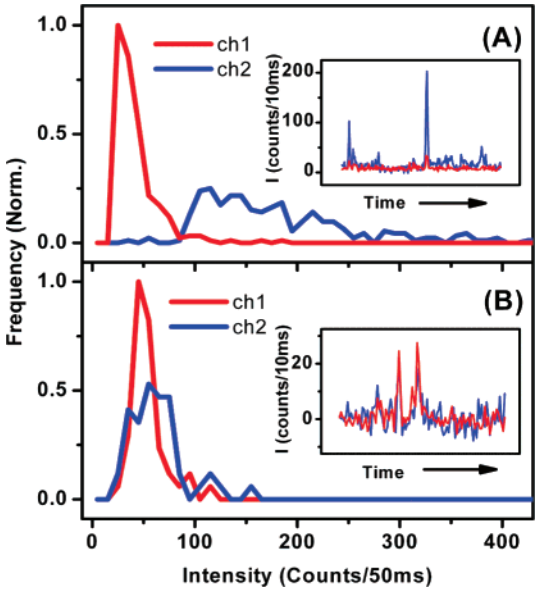

Figure 3. Dual-channel fluorescence intensity histograms of MEH-PPV in 5CB without (A) and with (B) an applied E-field at 3 μm from the LC−PVA interface. The insets show intensity bursts from single polymers diffusing through the focal volume.

of 10 V, the extinction of the transmittance indicates that the molecules in the bulk LC solution are aligned parallel to the E-field (perpendicular to the substrate), in the homeotropic alignment. MEH-PPV-doped 5CB devices showed similar electro-optical behavior, suggesting that the presence of a low concentration of MEH-PPV does not alter the orientation of the LC during the application of the E-field. All further experiments with applied E-fields were performed at $V = 10$ V (5.5×10^3 V/cm rms voltage).

We have previously shown that MEH-PPV molecules dissolved in 5CB are highly aligned, with an orientation order parameter approaching unity.[6−8] This is shown in Figure 2(A,C), in the form of a schematic drawing and a polarization histogram, respectively. In Figure 2(C), the experimental polarization histogram (scatter) is peaked at 0.68 with a standard deviation of 0.10. The single molecule polarization distribution is fit (line) using a conformational order parameter S_c (presenting the averaged conformation of a single polymer chain) of 0.70 and an orientation order parameter S_o (presenting the average orientation of the main polymer axis with respect to the LC director) of 0.99. The theoretical fit is based on an anisotropic mean field solvation model with the assumption that the shape of the polymer chain can be approximated as a cylinder, as described in previous work.[6,7] The effects of shot noise broadening and a high NA objective[39] are also considered in the fitting routine.

With an applied E-field, the experimental polarization distribution (scatter) measured at 3 μm inside the cell is now peaked at 0 with a standard deviation of 0.17 (Figure 2(D)), indicating a change in the orientation of the MEH-PPV molecules. A polarization histogram peaked at 0 is consistent with three scenarios: (1) a random alignment of fast rotating polymer chains (isotropic alignment), (2) a polymer conformation with spherical symmetry, and (3) anisotropic polymer chains that are perpendicularly aligned with respect to the substrate. An isotropic alignment of the MEH-PPV molecules can be ruled out considering that applying an E-field perpendicular to the substrate causes only a change of the LC director orientation without a change of the LC order parameter.[11,40,41]

In order to distinguish between a collapsed spherically symmetric conformation and a perpendicular alignment, the dual channel intensity histograms with and without an applied E-field are compared. The results of this comparison are shown in Figure 3 for a measurement at a depth of 3 μm from the LC−PVA interface without (A) and with (B) an applied E-field. The insets show intensity bursts of a single polymer freely diffusing through the focal volume. Channel 1 and channel 2 each detect one of the two orthogonal polarization components of the fluorescence emitted from within the sample plane. The sample is oriented such that, without an applied E-field, the LC director, and hence the long axes of the MEH-PPV molecules, are oriented parallel to the polarization detected by channel 2. In this case, the burst intensity is much higher in channel 2 compared to channel 1. In Figure 3(A), the mean intensities of channel 1 and channel 2 are 40 and 201 (counts/50 ms), respectively. In contrast, the burst intensities from the two channels are almost the same with the E-field applied to the LC cell. This is shown in Figure 3(B) where the mean intensities are 54 and 63 counts/50 ms for channel 1 and 2, respectively.

A spherically symmetric conformation can be ruled out by comparing the mean intensity of channel 1 and 2 using a simplified model without considering the effect of a high NA objective. The detected intensities of channel 1 and channel 2 depend on the conformation and orientation of the MEH-PPV molecules. In the absence of an external field, the MEH-PPV molecules are modeled as cylinders aligned parallel to the substrate as shown in Figure 2(A). The intensities of channel 2 ($I_{ch2,planar} = 201$ counts/50 ms) and channel 1 ($I_{ch1,planar} = 40$ counts/50 ms) measure the fluorescence emitted from the polymer segments in the sample plane parallel and perpendicular to the LC director, respectively. However, because of the collection geometry, fluorescence emitted from polymer chains oriented perpendicular to the substrate and hence polarized along the optical axis (I_z) cannot be detected. For a cylindrical polymer conformation, I_z equals to $I_{ch1,planar}$ and the total fluorescence intensity emitted from the polymer molecules is then $I_{total} = I_{ch1,planar} + I_{ch2,planar} + I_z$. Assuming that I_{total} is independent of polymer conformation, the intensities of channel 1 and 2 should be equal to $^1/_3(I_{ch1,planar} + I_{ch2,planar} + I_z)$ if the polymer conformation becomes spherically symmetric in the presence of an E-field. This calculation predicts an intensity of ~94 counts/50 ms for channel 1 and 2. However, this value is much

higher than the measured mean intensities of 54 and 63 counts/50 ms for channel 1 and 2, respectively. A spherically symmetric polymer conformation can therefore be ruled out. However, if the long axis of the polymer is aligned perpendicular to the substrate without a change of polymer conformation, the intensities of channel 1 and channel 2 should be equal to $I_{ch1,planar}$ (i.e., $I_{ch1,homeotropic} = I_{ch2,homeotropic} = 40$ counts/50 ms), which is in reasonable agreement with the measured mean intensities of 54 and 63 (counts/50 ms). The small shift toward higher values for the observed intensities is due to the high NA objective, which allows for small contributions from I_z to be detected.[39]

The measured polarization distribution with an applied E-field can therefore only be explained with a perpendicular alignment of MEH-PPV with respect to the device substrate. The polarization in Figure 2D is modeled with such a perpendicular alignment using the same conformational and orientation order parameters as in the case without an applied field. The fact that the same conformational order parameter can be used to model the measured polarization histogram suggests that the polymer chains are equally stretched in the homeotropic alignment compared to the planar alignment. This is in good agreement with the fact that the LC order parameter is unchanged regardless of the director orientation.[11,40,41] This implies that the individual polymer segments always experience the same solvation energy independent of director orientation, consistent with our experimental results. Furthermore, the good fit of the polarization histograms in Figure 2 verifies our model for the anisotropic alignment of polymer chains in a LC host and justifies the assumption made about a cylindrical polymer conformation. The results further support the previously introduced concept of *cooperative anisotropic solvation*. Because a MEH-PPV molecule is about 100 times larger than a 5CB molecule, each polymer experiences a solvation potential equal to that of many (~100) solvent molecules added together. The MEH-PPV molecules are therefore perfectly aligned with the nematic director as a result of this large cooperative anisotropic solvation energy, independent of an applied E-field.

However, how do the MEH-PPV molecules align in the vicinity of the device interface? It is well-known that the LC molecules near the device interface remain aligned parallel to the substrate because of strong interactions (i.e., surface anchoring) with a surface alignment layer. It is of interest to ascertain if the MEH-PPV molecules can probe this local nematic alignment. Figure 4 shows the polarization histograms for single MEH-PPV chains with field off (left column) and on (right column) for the laser focused at $Z = 0-3$ μm, where Z is the distance between the LC−PVA interface and the position of the laser focal point. In the absence of an applied field, the polarization histograms are almost identical and peaked at 0.68 for $Z = 0-3$ μm. When an AC E-field is applied, the peak of the polarization histogram shifts from 0.6 at $Z = 0$ μm to 0 at $Z > 2$ μm. At intermediate distances of $Z = 1$ and 1.5 μm, the polarization histograms are broad, reflecting a complex LC ordering in the transition region between the surface-aligned LC molecules and the electric field oriented bulk of the solution. In contrast, the peaks of the polarization histograms in the planar alignment (i.e., without external field) do not change as a function of depth (Figure 4, left column). This suggests that planar alignment is homogeneous independent of depth, which confirms that our LC device consists of a single domain nematic LC.[42] In addition, the absence of a change in the polarization distributions as a function of Z in the absence of an applied E-field also confirms that the LC birefringence has no effect on the fluorescence polarization in our experiments.

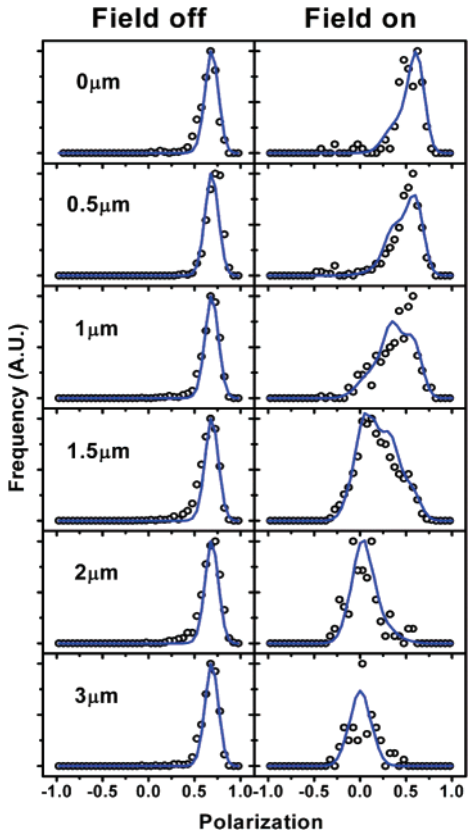

Figure 4. Polarization histograms measured using circularly polarized excitation with field off (left column, scatter) and field on (right column, scatter). The laser was focused at different distances from the LC−PVA interface, $Z = 0$, 0.5, 1, 1.5, 2, and 3 μm. The simulated polarization histograms (blue lines) for an applied E-field are modeled taking into account the depth dependence on the LC director orientation near the substrate interface based on an elastic model (see Figure 5 and text for details).

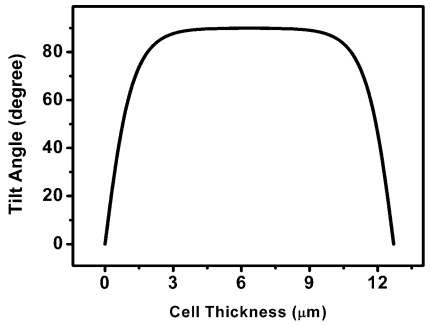

Figure 5. Tilt angle distribution as a function of distance from the LC−PVA interface calculated from Frank continuum theory.

The spatial director profile of the LC molecules with an external field is usually evaluated using Frank continuum theory,[11,37] where the deformation of the LC is described by a continuous elastic theory, considering the free energy of deformation of the LC and the effect of an electric field. When applying an external field of sufficient magnitude, the LC molecules form two structures: (1) a transition layer in which the LC director changes orientation continuously and (2) a bulk region where the director is perpendicular to the substrate.[11] Figure 5 shows the director profile as a function of depth from the interface calculated from Franck continuum theory. The tilt angle θ in Figure 5 is the angle between the LC director and the substrate. In the simulation, we choose the x-y plane as the substrate surface, the y-axis as the nematic director without applying an E-field (i.e., the rubbing direction of the alignment

layer), and the *z*-axis as the direction of the applied E-field. It is further assumed that the surface-anchoring energy is so strong that the tilt angle of the LC molecules at the cell surface is always 0° regardless of the magnitude of the E-field. For the Frank continuum theory, the free energy density of elastic deformation (f_d) and electric field (f_e) are given as:

$$f_d = \frac{1}{2}K_{11}(\nabla \cdot \hat{n})^2 + \frac{1}{2}K_{33}\{\hat{n} \times (\nabla \times \hat{n})\}^2 \quad (2)$$

$$f_e = \frac{1}{2}\epsilon_0\epsilon_a(\vec{E} \cdot \hat{n})^2 \quad (3)$$

K_{11} and K_{33} are the elastic constants for splay and bend deformation, $\hat{n}$ is the unit vector of the nematic director, ϵ_0 is the dielectric constant in vacuum, and ϵ_a is the difference of the dielectric constants along and normal to the nematic director. With $(n_y,n_z) = (\cos\theta(z),\sin\theta(z))$ and $\vec{E} \cdot \hat{n} = E \sin\theta$, the total free energy F_t is given by:

$$F_t = \int_0^d \frac{1}{2}\left\{(K_{11}\cos^2\theta(z) + K_{33}\sin^2\theta(z))\left(\frac{d\theta(z)}{dz}\right)^2 - \epsilon_0\epsilon_a E^2 \sin^2\theta(z)\right\}dz \quad (4)$$

where d is the thickness of the cell. The director profile is obtained by minimizing F_t with respect to θ using on an iterative finite-difference method.[43] The result for an E-field of $\sim 5.5 \times 10^3$ V/cm applied to a 5CB nematic device with a thickness of 12.7 μm is shown in Figure 5.

Using the director profile shown in Figure 5, obtained from Frank continuum theory, we simulate the polarization histogram for MEH-PPV in 5CB as a function of distance from the LC device interface. For the simulation, it is assumed that the LC device is divided into 127 layers with a thickness of 0.1 μm. In each layer the director orientation is assumed to be constant. The polarization histogram in a single layer is simulated for the same polymer conformation as above (i.e., $S_c = 0.70$) aligned in the microscope plane and then rotated to match the director orientation in that specific layer. The total polarization histogram in the focal volume with a height of 2.2 μm is obtained using:

$$P_{total}(a) = N\left(C\sum_{n=0}^{9}\exp\left(-\frac{2(0.1n-a)^2}{1.1^2}\right)P(0.1n) + \sum_{n=10}^{127}\exp\left(-\frac{2(0.1n-a)^2}{1.1^2}\right)P(0.1n)\right) \quad (5)$$

$P_{total}(a)$ is the total polarization distribution collected from MEH-PPV molecules in the focal volume of a Gaussian beam focused at a depth of a μm. $P(0.1n)$ is the polarization distribution of a single layer at a depth of $0.1n$ μm. N is the normalization factor and $C = 5$ is the correction factor for the detection sensitivity.[44] The simulated polarization histograms are shown as blue lines in the right column of Figure 4. The simulated (line) and measured (scatter) polarization distributions agree very well and demonstrate that the MEH-PPV molecules follow the orientation of the LC director as expected from our discussion above, and that the director profile is correctly modeled by Franck continuum theory. MEH-PPV therefore acts as a probe of the local structure in our LC devices and can possibly be used to explore more complex anisotropic media.

It is interesting to compare the diffusion of MEH-PPV near the surface for the E-field switched on vs switched off. Figure 6 shows the autocorrelation of MEH-PPV in 5CB with field off (blue) and field on (red) at $Z = 0.5$ μm. The autocorrelation function is calculated from the MEH-PPV molecules that show a polarization larger than 0.2, i.e., only molecules that are not aligned perfectly perpendicular to the substrate are included. In Figure 6 the autocorrelation function with the E-field switched on shows a faster decay than the one with the E-field switched off, suggesting a shorter diffusion time for the MEH-PPV molecules diffusing through the focal volume when an E-field is applied. It has been reported that the viscosity of 5CB is increased near the substrate interface with an applied E-field.[45,46] However, an increase in the local viscosity would imply a slower diffusion of the MEH-PPV molecules, which is contradictory to our observation. Changes in the autocorrelation due to interface-induced quenching of the MEH-PPV can also be ruled out by comparing the fluorescence intensity histograms measured for different focal positions Z and with the field on vs field off.

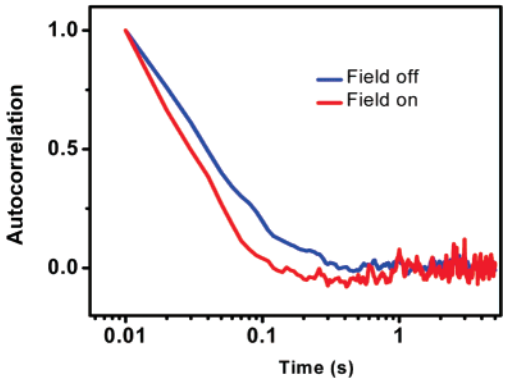

Figure 6. Autocorrelation function of MEH-PPV diffusing in 5CB measured at $Z = 0.5$ μm with (red) and without (blue) an applied E-field.

Another possible explanation is a change in the "effective focal volume" causing the apparent diffusion time to be faster. None of our experiments suggest that the actual laser focal volume is much smaller with an applied E-field (ignoring small changes due to orientation dependent LC refractive indices). However, the polymer molecules that are oriented perpendicular to the substrate are less likely to be excited because with increasing distance away from the LC device interface, their absorption dipole moments are tilted toward the laser light propagation direction. When the MEH-PPV molecules diffuse vertically away from the substrate into the bulk solvent region while an E-field is applied, they change orientation from a mainly planar alignment with a large absorption probability to a homeotropic alignment with a much smaller absorption probability. The further the MEH-PPV molecules diffuse away from the interface the smaller their contribution to the autocorrelation signal becomes because of a smaller absorption probability. Without an applied field, the MEH-PPV molecules give rise to the same absorption probability even if they diffuse vertically. As a result, the autocorrelation samples a smaller effective region with an applied E-field resulting in a shorter diffusion time as shown in Figure 6. When the E-field is turned on, the effective focal volume for $Z = 0.5$ μm decreases because of the smaller apparent depth in the *z*-axis. Consistent with this explanation is also the fact that, independent of an applied E-field, no change in the autocorrelation function is observed at $Z = 3$ μm with a diffusion time comparable to the measurement at $Z = 0.5$ μm without an E-field.

Based on the diffusion analysis, the measurable depth in the *z*-axis is 617 ± 217 nm assuming no change in diffusion

constant for MEH-PPV. In the autocorrelation measurement, we select molecules with polarization values larger than 0.2 corresponding to a molecular tilt angle smaller than 51°. For the simulated tilt angle distribution in Figure 5, molecules within 800 nm from the LC substrate interface have tilt angles smaller than 51°. The diffusion analysis is therefore also consistent with the Frank continuum theory.

Conclusion

We have investigated the alignment of a polymer solute with respect to the LC director in a LC device while applying an external electric field. The experiments demonstrate that with an external E-field of 5.5×10^3 V/cm the MEH-PPV molecules are aligned perpendicular to the device substrate in the bulk of the LC without a change of polymer conformation. These results are consistent with our previous model of cooperative anisotropic solvation that describes the high degree of solute alignment with respect to the LC director for the long, stiff MEH-PPV polymer chains in an anisotropic solvent. The E-field studies further imply that it is possible to switch the MEH-PPV alignment by controlling the direction of the anisotropic solvation potential through an E-field. The observed variation of the polarization histogram with distance away from the device interface results from a continuous field-induced deformation of the LC director near the device interface and can be described by a conventional elastic model. The depth-dependent orientation of the MEH-PPV quantitatively matches the director profile that was obtained independently by Frank continuum theory. These results therefore suggest that MEH-PPV can be used as a probe to unveil the complex local structure in a LC.

Acknowledgment. This material is based upon work supported by the National Science Foundation under Grant No. CHE-0416112 to P.F.B. and Grant No. CHE-0315219 to A.Y. P.F.B. acknowledges support from the Keck Foundation and the Welch Foundation.

References and Notes

(1) Hoeben, F. J. M.; Jonkheijm, P.; Meijer, E. W.; Schenning, A. *Chem. Rev.* **2005**, *105*, 1491.
(2) Hulvat, J. F.; Stupp, S. I. *Angew. Chem., Int. Ed.* **2003**, *42*, 778.
(3) Hulvat, J. F.; Stupp, S. I. *Adv. Mater.* **2004**, *16*, 589.
(4) Kato, T.; Mizoshita, N.; Kishimoto, K. *Angew. Chem., Int. Ed.* **2006**, *45*, 38.
(5) Dogic, Z.; Zhang, J.; Lau, A. W. C.; Aranda-Espinoza, H.; Dalhaimer, P.; Discher, D. E.; Janmey, P. A.; Kamien, R. D.; Lubensky, T. C.; Yodh, A. G. *Phys. Rev. Lett.* **2004**, *92*, 125503.
(6) Link, S.; Hu, D.; Chang, W. S.; Scholes, G. D.; Barbara, P. F. *Nano Lett.* **2005**, *5*, 1757.
(7) Link, S.; Chang, W. S.; Yethiraj, A.; Barbara, P. F. *Phys. Rev. Lett.* **2006**, *96*.
(8) Lammi, R. K.; Fritz, K. P.; Scholes, G. D.; Barbara, P. F. *J. Phys. Chem. B* **2004**, *108*, 4593.
(9) Fritz, K. P.; Scholes, G. D. *J. Phys. Chem. B* **2003**, *107*, 10141.
(10) Onsager, L. *Ann. N. Y. Acad. Sci.* **1949**, *51*, 627.
(11) de Gennes, P. G. a. P., J *The Physics of Liquid Crystal*, 2nd ed.; Oxford Science Publications: 1993.
(12) Boichuk, V.; Kucheev, S.; Parka, J.; Reshetnyak, V.; Reznikov, Y.; Shiyanovskaya, I.; Singer, K. D.; Slussarenko, S. *J. Appl. Phys.* **2001**, *90*, 5963.
(13) Bryan-Brown, G. P.; Wood, E. L.; Sage, I. C. *Nature* **1999**, *399*, 338.
(14) Presnyakov, V. V.; Galstian, T. V. *J. Appl. Phys.* **2005**, *97*.
(15) Tadokoro, T.; Toriumi, H.; Okutani, S.; Kimura, M.; Akahane, T. *Jpn. J. Appl. Phys., Part 1* **2003**, *42*, 4552.
(16) Ekgasit, S.; Fulleborn, M.; Siesler, H. W. *Vib. Spectrosc.* **1999**, *19*, 85.
(17) Fukazawa, T.; Tadokoro, T.; Toriumi, H.; Akahane, T.; Kimura, M. *Thin Solid Films* **1998**, *313*, 799.
(18) Mitsuishi, M.; Ito, S.; Yamamoto, M.; Fischer, T.; Knoll, W. *J. Appl. Phys.* **1997**, *81*, 1135.
(19) Noble, A. R.; Kwon, H. J.; Nuzzo, R. G. *J. Am. Chem. Soc.* **2002**, *124*, 15020.
(20) Noble-Luginbuhl, A. R.; Blanchard, R. M.; Nuzzo, R. G. *J. Am. Chem. Soc.* **2000**, *122*, 3917.
(21) Okutani, S.; Kimura, M.; Toriumi, H.; Akao, K.; Tadokoro, T.; Akahane, T. *Jpn. J. Appl. Phys., Part 1* **2001**, *40*, 244.
(22) Shilov, S. V.; Okretic, S.; Siesler, H. W. *Vib. Spectrosc.* **1995**, *9*, 57.
(23) Smith, N. J.; Sambles, J. R. *Appl. Phys. Lett.* **2000**, *77*, 2632.
(24) Smith, N. J.; Tillin, M. D.; Sambles, J. R. *Phys. Rev. Lett.* **2002**, *88*.
(25) Tadokoro, T.; Fukazawa, T.; Toriumi, H. *Jpn. J. Appl. Phys., Part 2* **1997**, *36*, L1207.
(26) Toriumi, H.; Akahane, T. *Jpn. J. Appl. Phys., Part 1* **1998**, *37*, 608.
(27) Yang, F. Z.; Ruan, L. Z.; Sambles, J. R. *J. Appl. Phys.* **2000**, *88*, 6175.
(28) Yang, C. L.; Chen, S. H. *Jpn. J. Appl. Phys., Part 1* **2002**, *41*, 3778.
(29) Smalyukh, II; Shiyanovskii, S. V.; Lavrentovich, O. D. *Chem. Phys. Lett.* **2001**, *336*, 88.
(30) Lavrentovich, O. D. *Pramana* **2003**, *61*, 373.
(31) Gheorghiu, N.; Smalyukh, II; Lavrentovich, O. D.; Gleeson, J. T. *Phys. Rev. E* **2006**, *74*.
(32) Dierking, I. *ChemPhysChem* **2001**, *2*, 663.
(33) Ozaki, R.; Aoki, M.; Moritake, H.; Yoshino, K.; Toda, K. *Jpn. J. Appl. Phys., Part 1* **2006**, *45*, 4662.
(34) Moritake, H.; Kim, J.; Toda, K.; Yoshino, K. *Mol. Cryst. Liq. Cryst.* **2005**, *436*, 1201.
(35) Moritake, H.; Kim, J.; Yoshino, K.; Toda, K. *Jpn. J. Appl. Phys., Part 1* **2005**, *44*, 4316.
(36) Moritake, H.; Kim, J.; Yoshino, K.; Toda, K. *Jpn. J. Appl. Phys., Part 1* **2004**, *43*, 6780.
(37) Frank, F. C. *Discuss. Faraday Soc.* **1958**, *29*, 19.
(38) Sugimura, A.; Ishino, D.; Matsumoto, K.; Ishihara, S. *Mol. Cryst. Liq. Cryst.* **2003**, *400*, 97.
(39) Forkey, J. N.; Quinlan, M. E.; Goldman, Y. E. *Prog. Biophys. Mol. Biol.* **2000**, *74*, 1.
(40) Lelidis, I.; Nobili, M.; Durand, G. *Phys. Rev. E* **1993**, *48*, 3818.
(41) Mottram, N. J.; Hogan, S. J. *Continuum Mech. Thermodyn.* **2002**, *14*, 281.
(42) Chigrinov, V. G. *Liquid Crystal Devices: Physics and Applications*; Artech House: Boston, 1999.
(43) Wang, Q.; He, S. L.; Yu, F. H.; Huang, N. R. *Opt. Eng.* **2001**, *40*, 2552.
(44) The correction factor for the detection sensitivity is calculated as the ratio of the averaged blip intensity with the E-field switched on and off at focus position of Z = 3 micrometer.
(45) Negita, K. *J. Chem. Phys.* **1996**, *105*, 7837.
(46) Ozaki, R.; Aoki, M.; Moritake, H.; Yoshino, K.; Toda, K. *Jpn. J. Appl. Phys., Part 1* **2006**, *45*, 4662.